

## Tight-binding description of the electronic structure and total energy of tin

BRAHIM AKDIM<sup>†§</sup> D. A. PAPACONSTANTOPOULOS<sup>†‡</sup> and M. J. MEHL<sup>‡||</sup>

<sup>†</sup> Institute for Computational Sciences and Informatics, George Mason University, Fairfax, Virginia 22030, USA

<sup>‡</sup> Center for Computational Materials Science, Naval Research Laboratory, Washington, DC 20375-5345, USA

[Received 3 May 2001 and accepted 23 May 2001]

### ABSTRACT

The Naval Research Laboratory (NRL) tight-binding (TB) method was applied to tin, a material which is known to exist in the diamond structure ( $\alpha$ -Sn) at zero temperature and low pressures. A small change in the pressure drives tin to the  $\beta$ -Sn structure, which is stable up to 9.5 GPa at room temperature. In this paper we present the NRL-TB parameterization for tin, applying it to the study of the bulk properties of both  $\alpha$ -Sn and  $\beta$ -Sn. The parameters were determined by fitting to a database of first-principles band structures and total energies, generated using the general potential linearized augmented plane-wave method for the fcc, bcc, sc and diamond structures, with limited information from calculations of the  $\beta$ -Sn phase. We report the success of this method in predicting the two stable structures  $\alpha$ -Sn and  $\beta$ -Sn in the correct order, even though these structures have a small energy difference. We also discuss the NRL-TB method's ability to calculate electronic band structures and density of states. We confirm the semimetallic and metallic character for the  $\alpha$ -Sn and bcc phases respectively. We also calculate the elastic constants of  $\alpha$ -Sn and  $\beta$ -Sn, as well as several high-symmetry point phonon frequencies of  $\alpha$ -Sn and compare our results with experiment. Finally, TB molecular dynamics calculations are used to explore the behaviour of tin at finite temperatures. We compute the temperature dependence of the Debye–Waller  $B$  factor, finding it to be consistent with experiment up to room temperature.

### § 1. INTRODUCTION

Tin has the atomic number  $Z = 50$  and four electrons in the valence band. The ground state, grey tin ( $\alpha$ -Sn), has the diamond structure (Villars and Calvert 1991), in common with the lighter elements in column IV A of the periodic table. Tin also exists in the  $\beta$ -Sn structure (white tin) at atmospheric pressure above 13°C. The  $\beta$ -Sn phase (space group,  $I4_1/amd$ ; Pearson symbol,  $tI4$ ; *Strukturbericht* designation, A5) is a tetragonal distortion of diamond with two atoms per unit cell¶. It is stable up to 9.5 GPa at room temperature, where it transforms to a bct form, followed by a transformation to the cubic bcc structure (Olijnyk and Holzapfel 1984,

§ Current address: Ohio Supercomputer Center, Columbus, Ohio 43212, USA

|| Author for correspondence. Email: mehl@dave.nrl.navy.mil

¶ For more information about the  $\beta$ -Sn structure, see <http://cst-www.nrl.navy.mil/lattice/struk/a5.html>.

Desgreniers *et al.* 1989, Villars and Calvert 1991). These temperature- and pressure-driven phase transformations have caused tin to be of considerable experimental and theoretical interest.

Christensen and Methfessel (1993) performed *ab initio* calculations using the full-potential (FP) linear muffin-tin orbital (LMTO) method. They reported all the transitions sequence observed experimentally,  $\alpha$ -Sn  $\rightarrow$   $\beta$ -Sn  $\rightarrow$  bct  $\rightarrow$  bcc. For large systems, computations using FP-LMTO or any other self-consistent first-principles method are slow, and a faster method is desirable. In this paper we use the Naval Research Laboratory (NRL) tight-binding (TB)<sup>†</sup> (Cohen *et al.* 1994, Mehl and Papaconstantopoulos 1996, Kirchhoff *et al.* 2001) procedure to map the results of a database of first-principles calculations on to a set of TB parameters, which can then be used to determine the mechanical and electronic properties of arbitrary structures. The NRL-TB method has been successfully used for a variety of materials, including the transition metals (Mehl and Papaconstantopoulos 1996), sp metals (Yang *et al.* 1994), and the semiconductors carbon and silicon (Papaconstantopoulos *et al.* 1998, Bernstein *et al.* 2000). The elastic moduli, equilibrium lattice constant, vacancy formation energy, surface energy and phonon spectra predicted by these parameters were found to be in very good agreement with experiment. In the present work, we take the same approach to study the bulk properties of tin, which is known to be a semiconductor with a zero bandgap (semimetal) in the  $\alpha$ -Sn phase, and a metal in the  $\beta$ -Sn, bct and bcc structures (Donohue 1974).

This paper is structured as follows: we outline the theory of the NRL-TB method in §2, describe the numerical methods used in the first-principles and the NRL-TB calculations in §3, present our results and discussion in §4 and conclude with a summary in §5.

## §2. THEORY

The aim of the NRL-TB method is twofold: first, to reproduce the electronic-band structure of a system as was done in earlier TB work (Papaconstantopoulos 1986), together with the total energy of the system; second, to make sure that these parameters are transferable from one structure to another. To do this, we use the two-centre formalism of Slater and Koster (SK) (1954), including environmentally sensitive on-site terms. This section describes the procedure in some detail.

We begin with the expression of the total energy found in density functional theory (Hohenberg and Kohn 1964, Kohn and Sham 1965):

$$E[n(\mathbf{r})] = \sum_{\text{occ}} \epsilon_n + F[n(\mathbf{r})] \quad (1)$$

where the first term is a sum over the occupied single-particle Kohn–Sham orbitals and  $F$  represents the remaining terms of the total energy that depend on the charge density  $n(\mathbf{r})$ . We note that there is a certain ambiguity in the values of the two terms, since the Kohn–Sham potential can be uniformly shifted by an arbitrary constant. We eliminate this ambiguity by defining a particular shift

$$V_0(S, a) = \frac{F[n(\mathbf{r})]}{N_e}, \quad (2)$$

---

<sup>†</sup> The TB parameters and computer codes used in this paper are available from the DoD Tight-Binding Home Page, <http://cst-www.nrl.navy.mil/bind/dodtb>.

where  $N_e$  is the number of electrons. Note that  $V_0$  depends on the structure  $S$  and lattice parameters  $a$ . Shifting the eigenvalues by  $V_0$  allows us to write the total energy as

$$E[n(r)] = \sum_{\text{occ}} \epsilon'_n, \quad (3)$$

where  $\epsilon'_n = \epsilon_n + V_0$ . The result is that the sum of the shifted eigenvalues is equal to the total energy, and therefore we need only concern ourselves with the shifted eigenvalues when deriving our TB parameters. Our goal is to construct a non-orthogonal (TB) Hamiltonian whose eigenvalues are the  $\epsilon'_i$ :

$$\mathbf{H} - \epsilon' \mathbf{S} = 0, \quad (4)$$

where the matrix elements of  $\mathbf{H}$  and  $\mathbf{S}$  are derived from the two-centre SK parameters (Slater and Koster 1954, Papaconstantopoulos 1986), which include on-site terms, hopping integrals and overlap integrals. For tin we use only the 5s and 5p orbitals on each atom to construct the TB basis.

In the NRL-TB method we construct the on-site parameters of  $\mathbf{H}$  so that they are diagonal and sensitive to the local environment (Sigalas and Papaconstantopoulos 1994, Mehl and Papaconstantopoulos 1995, 1996). We write the on-site term of the orbitals with angular momentum  $\ell$  of atom  $i$  as

$$h_{i\ell}(\rho_i) = \alpha_\ell + \beta_\ell \rho_i^{2/3} + \gamma_\ell \rho_i^{4/3} + \delta_\ell \rho_i^2, \quad (5)$$

where  $\ell$  is an angular momentum index and  $\rho_i$  is a fictitious atomic-like density which monitors the distribution of neighbouring atoms:

$$\rho_i = \sum_{j \neq i} \exp(-\lambda^2 R_{ij}) F_c(R_{ij}). \quad (6)$$

Here  $\lambda$ ,  $\alpha_\ell$ ,  $\beta_\ell$ ,  $\gamma_\ell$  and  $\delta_\ell$  are new parameters which are to be determined by fitting to first principles calculations and  $R_{ij}$  is the distance between atoms  $i$  and  $j$ .  $F_c$  is a smooth cut-off function that restricts the calculation to about five shells of neighbouring atoms:

$$F_c(r) = \{1 + \exp[(r - r_0)L^{-1}]\}^{-1}. \quad (7)$$

In these calculations we use  $r_0 = 14$  Bohr and  $L = 0.5$  Bohr.

Within the non-orthogonal two-centre approximation we must specify the form of both the SK hopping and the overlap integrals. We assume that these depend only on the nature of the bonding orbital and the distance between the two atoms. For the hopping integrals we take

$$P_i(r) = (a_i + b_i r + c_i r^2) \exp(-d_i^2 r) F_c(r), \quad (8)$$

where  $F_c$  is the same as in equation (7) and  $r$  is the distance between the atoms. We write the overlap matrix elements in a similar form:

$$P'_i(r) = (a'_i + b'_i r + c'_i r'^2) \exp(-d_i'^2 r) F_c(r). \quad (9)$$

For tin we shall only consider the sp basis of the valence atoms; so  $P_i$  and  $P'_i$  represent the interactions  $ss\sigma$ ,  $sp\sigma$ ,  $pp\sigma$ , and  $pp\pi$ . The parameters  $a_i$ ,  $b_i$ ,  $c_i$ ,  $d_i$ ,  $a'_i$ ,  $b'_i$ ,  $c'_i$  and  $d'_i$  are chosen to reproduce the results of a database of first-principles calculations, as outlined below.

### §3. COMPUTATIONAL DETAILS

#### 3.1. *Linearized augmented plane-wave calculations*

In order to create a database for the TB method we performed a set of FP linearized augmented plane-wave (LAPW) (Andersen 1975, Koelling and Arbmán 1975, Wei and Krakauer 1985) calculations. In these calculations, we used a muffin-tin sphere radius  $R_{\text{MT}}$  of 2.0 Bohr. This is small enough that the muffin-tin spheres do not overlap for any of our calculations, but large enough that no more than 0.05% of the 4s and 4p core electrons are outside the muffin-tin sphere. These FP calculations were carried out using a cut-off  $K_{\text{max}} R_{\text{MT}} = 8.5$  to determine the size of the secular equation, where  $K_{\text{max}}$  is the magnitude of the largest  $\mathbf{k}$  vector. The above parameters were kept fixed throughout the calculations for all the structures. We used a regular mesh with 89  $\mathbf{k}$  points in the irreducible Brillouin zone for the fcc and  $\alpha$ -Sn structures. In the sc and bcc structures we used regular meshes with 35 and 55  $\mathbf{k}$  points respectively in the irreducible Brillouin zone. The band calculations are semi-relativistic, with no spin-orbit splitting (Koelling and Harmon 1977), while the core levels are treated fully relativistically. Except as noted below, the exchange and correlation follow the Hedin-Lundqvist (1971) prescription.

We included the 4d semicore states of tin in the semirelativistic valence band, including localized basis functions (Singh 1991). These states, although low in energy and below the nominal  $sp^3$  valence states, have charge densities that reach out far enough into the outer part of the muffin-tin spheres that their effect cannot be ignored. The semicore electronic contribution is especially important when the crystal structures are known to be close in energy.

#### 3.2. *Tight-binding calculations*

In our TB method, as outlined in §2, we first fitted the SK parameters to LAPW results from four crystal structures, namely fcc, bcc and sc structures using four bands (one s and three p) for each  $\mathbf{k}$  point, and the diamond structure fitting eight bands at each  $\mathbf{k}$  point. We refer to these calculations as case 1. These calculations were performed with a non-orthogonal Hamiltonian in the two-centre approximation, using a total of 41 parameters to be optimized: nine parameters for the on-site terms (equation (5)), 16 parameters for the hopping integrals (equation (8)) and 16 parameters for the overlap integrals (equation (9)). The rms errors obtained in our fit are 1 mRy for the total energy and 25 mRy for the bands.

The case-1 parameters produce highly accurate electronic band structures for  $\alpha$ -Sn. However, using these parameters we found that the  $\beta$ -Sn structure was lower in energy than  $\alpha$ -Sn, contrary to experiment. This is not necessarily a failure of the TB method, as this behaviour has been seen in FP all-electron calculations (Christensen and Methfessel 1993)†. To check our results, we made a limited number of LAPW calculations for the  $\beta$ -Sn phase and found that this structure was lower than  $\alpha$ -Sn when using the Hedin-Lundqvist (1971) local density approximation parametrization. Interestingly, our calculations using a generalized gradient approximation (GGA) (Perdew 1991) density functional show the  $\beta$ -Sn phase to be higher in energy. We shall discuss this behaviour in detail in a future paper.

---

† In that case, the correct ordering was only obtained by adjusting the position of the 4d states within the FP LMTO calculation.

We developed a ‘case-2’ set of TB parameters to take these results into account. We fit to the same LAPW results as above but shifted the total energy of the diamond phase to reproduce the GGA energy difference between  $\alpha$ - and  $\beta$ -Sn at the experimental  $\beta$ -Sn volume. As we shall see below, these parameters are good for studying the structural properties of tin. Unfortunately, they do not produce good electronic band structures. We shall therefore use the case-1 parameters to study the electronic behaviour of tin, and the case-2 parameters to study structural behaviour.†

## §4. RESULTS AND DISCUSSION

### 4.1. Equation of state

Figure 1 shows the phase diagram resulting from our case-2 TB parameters. These parameters give the correct lattice equilibrium (table 1) and bulk modulus (table 2) of both the  $\alpha$ -Sn and  $\beta$ -Sn phases. Using these parameters, the equilibrium  $\beta$ -Sn phase unit cell is 12% smaller in volume than the equilibrium  $\alpha$ -Sn unit cell, in good agreement with the 10% reduction measured experimentally. The energy difference of 0.6 mRy between the  $\alpha$  and  $\beta$  phases compares favourably with the value of 0.7 mRy found by Christensen and Methfessel (1993). Also note that the  $\alpha$ -Sn structure is lower in energy than any other structure, in agreement with the experimental result showing that the diamond structure is the ground state of tin.

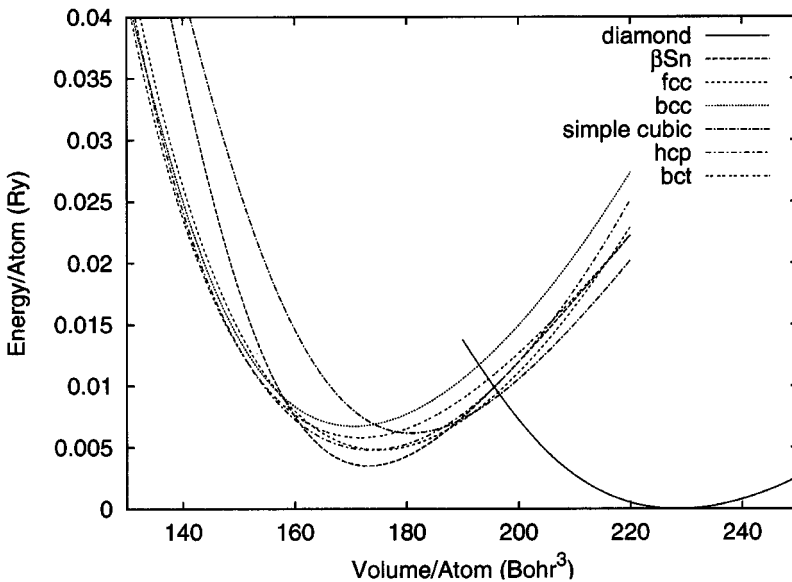


Figure 1. Tin phase diagram of case 2. 1 Bohr is the radius of the electron orbital in the Bohr model of the hydrogen atom and is equal to  $0.529 \times 10^{-10}$  m. 1 Rydberg is the binding energy of an electron in a hydrogen atom and is equal to 13.606 eV.

†Both sets of TB parameters are available from the World-Wide Web at <http://cst-www.nrl.navy.mil/bind/sn.html>.

Table 1. A comparison of the equilibrium lattice parameters of various structures for tin. TB refers to our case-2 TB parameters.

Structure	$a_0$ (Bohr)	$c/a$	Method
$\alpha$ -Sn	12.23		LAPW
	12.24		TB
	12.376		Other <sup>a</sup>
	12.263		Experiment <sup>b</sup>
$\beta$ -Sn	10.94	0.54	LAPW
	10.95	0.53	TB
	11.08	0.54	Other <sup>a</sup>
	11.019	0.5455	Experiment <sup>b</sup>
Fcc	8.856		LAPW
	8.898		TB
	8.995		Other <sup>a</sup>
Hcp	6.215	1.65	TB
	6.346	1.628	Other <sup>a</sup>
Bcc	7.03		LAPW
	7.02		TB
	7.09		Other <sup>a</sup>
Sc	5.695		LAPW
	5.71		TB
	5.778		Other <sup>a</sup>

<sup>a</sup>Christensen and Methfessel (1993).

<sup>b</sup>Villars and Calvert (1991).

Table 2. A comparison of the bulk moduli computed for various possible structures of tin. Calculations are performed at the experimental room temperature volume, if one is available. Otherwise, the calculations are performed at the LAPW equilibrium volume described in table 1, or the equilibrium volume from Christensen and Methfessel (1993).

Structure	Bulk modulus (GPa)			
	LAPW	TB	Other <sup>a</sup>	Experiment
$\alpha$ -Sn	45	45	51	53 <sup>a</sup>
$\beta$ -Sn		66		58 <sup>b</sup>
Fcc	63	51		
Hcp		22	62	
Bcc	58	57		
Sc	57	75		

<sup>a</sup>Christensen and Methfessel (1993).

<sup>b</sup>Simmons and Wang (1971).

The bulk properties resulting from case-2 calculations are summarized in table 2. Our TB results were compared with LAPW, LMTO (Christensen and Methfessel 1993) and experimental values (when available). The agreement is very good.

Our results for the hcp structure are comparable with the FP-LMTO results of Christensen and Methfessel (1993). For the other structures, fcc, bcc and sc, the obtained bulk results are comparable between LAPW, TB and LMTO methods.

A close examination of figure 1 shows that we correctly predict the phase transitions of tin in the  $\alpha$ -Sn  $\rightarrow$   $\beta$ -Sn  $\rightarrow$  bct sequence. We find that the  $\alpha \rightarrow \beta$  transition occurs at 1 GPa. Note that at room temperature this transition occurs just below 1 GPa; so we are in good agreement with the experiment value. The volume change at the transition is 23%, in good agreement with the experimental value. We also find evidence of a  $\beta$ -Sn  $\rightarrow$  bct phase transition at 20 GPa, with a volume change of 18%. This is significantly higher than the experimental value of 9.5 GPa. The bcc and bct structures are comparable at pressures above about 10 GPa; so it is difficult to say where, or whether, the bct  $\rightarrow$  bcc phase transition takes place using our TB binding parameters.

#### 4.2. Electronic structure

Figure 2 shows both the LAPW and the TB band structures of the  $\alpha$ -Sn phase at the calculated equilibrium lattice constant  $a_0 = 12.23$  Bohr using the case-1 TB parameters. These results are consistent with the fact that  $\alpha$ -Sn is a semimetal. There is good agreement between LAPW and TB valence bands, except that the lowest state at  $\Gamma$  is too high for the TB parameters. As is usual with semiconductors, an sp TB Hamiltonian does not reproduce the conduction band as accurately as the valence band (Bernstein *et al.* 2000).

The total densities of states (DOSs) for both the LAPW and the TB calculations of the  $\alpha$ -Sn structure at  $a_0 = 12.23$  Bohr are presented in figure 3. The lowest-energy peak is of s-like character. The second peak is a mix of s and p states and the remaining peaks, which bracket the Fermi level, have p-like character. In both methods we obtained very small DOSs near the Fermi energy. These features present strong similarities to silicon (Papaconstantopoulos 1986, Bernstein *et al.* 2000).

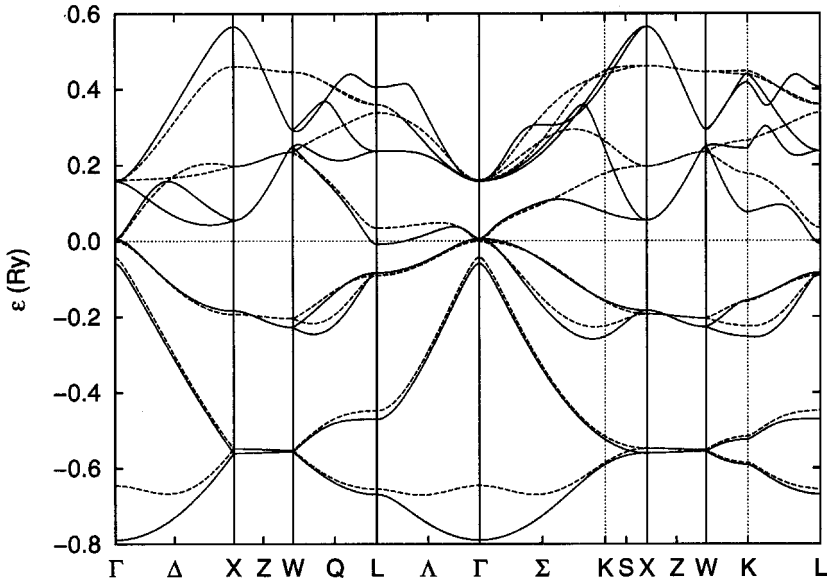


Figure 2. Band structure of diamond structure tin ( $\alpha$ -Sn) at the experimental lattice constant, 12.23 Bohr ( $1 \text{ Bohr} = 0.529 \times 10^{-10} \text{ m}$ ): (—), first-principles LAPW calculations; (- - -), TB results. In both calculations we set the Fermi level to zero. The energies are in rydberg ( $1 \text{ Ry} = 13.606 \text{ eV}$ ).

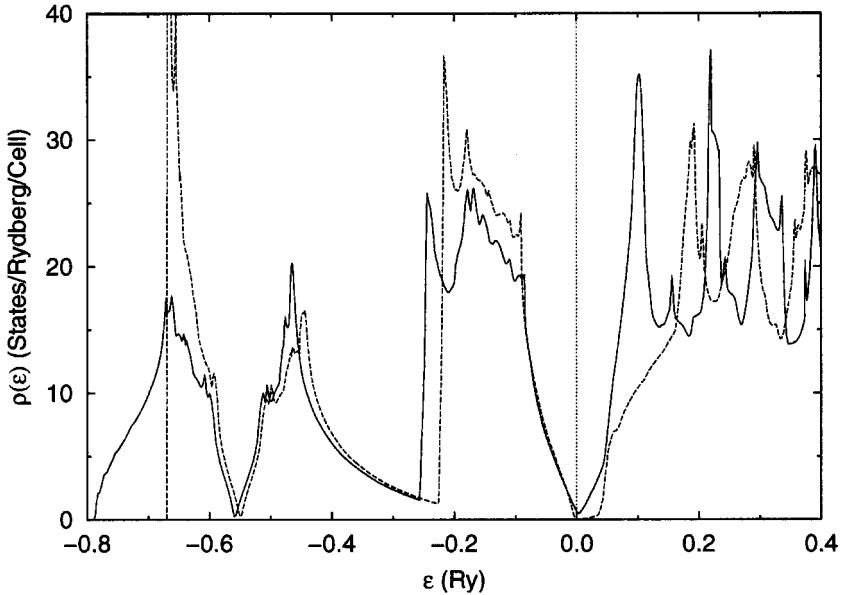


Figure 3. Electronic DOSs of diamond structure tin ( $\alpha$ -Sn) at the experimental lattice constant (12.23 Bohr): (—), first-principles LAPW calculations; (- - -), TB results. In both calculations we set the Fermi level to zero.

Figure 4 shows the bcc LAPW and TB band structures at the calculated equilibrium lattice constant ( $a_0 = 7.02$  Bohr), again using the case-1 parameters. Under pressure, the Fermi level crosses the bands, showing the metallic character observed experimentally. The bcc LAPW and TB DOSs are presented in figure 5, again at the calculated equilibrium lattice constant.

#### 4.3. Elastic constants and phonon frequencies

The elastic constants for the  $\alpha$  and  $\beta$  phases of tin were calculated from the case-2 TB parameters, as were selected phonon frequencies of  $\alpha$ -Sn. As noted above, these parameters give better mechanical properties for tin, at the expense of less accurate band structure properties.

The bulk modulus is determined from the energy  $E(V)$ , which is found by fixing the volume of the unit cell and adjusting all the free lattice parameters and internal parameters to minimize the total energy at that volume. Then

$$B(V) = -VP'(V) = VE''(V). \quad (10)$$

Here we determine  $B(V)$  by fitting  $E(V)$  to a Birch (1978)-like equation of state (Mehl 1993, Mehl *et al.* 1994) and differentiating that analytic equation.

The method for obtaining the other elastic constants has been described by Mehl (1993) and Mehl *et al.* (1994); for a given crystal structure, we calculate the energy as a function of the elastic strain components  $e_i$  ( $i = 1, \dots, 6$ ). The elastic constants are the second-order coefficients of an expansion of the energy in terms of the  $e_i$ :

$$E(\{e_i\}) = E(0) - PV \sum_{i=1}^3 e_i + \frac{1}{2} V \sum_{i=1}^6 \sum_{j=1}^6 C_{ij} e_i e_j + O[e_i^3], \quad (11)$$

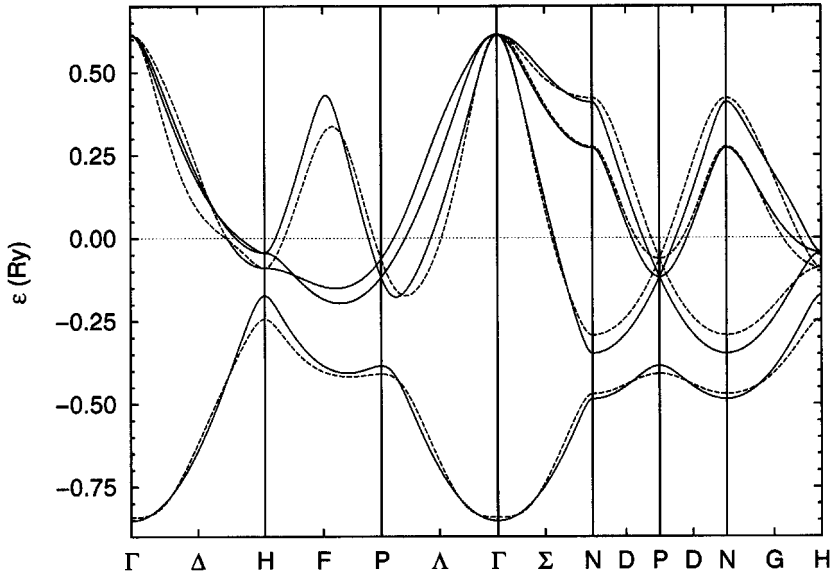


Figure 4. Band structure of bcc tin at the lattice constant  $a = 7.02$  Bohr: (—), first-principles LAPW calculations; (- - -), TB results. In both calculations we set the Fermi level to zero.

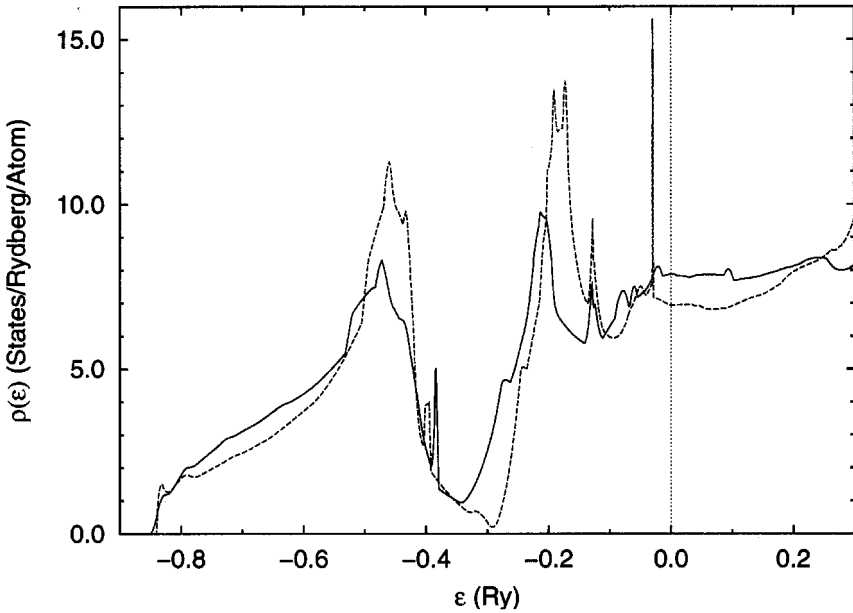


Figure 5. Electronic DOSs of bcc tin at the lattice constant  $a = 7.02$  Bohr: (—), first-principles LAPW calculations; (- - -), TB results. In both calculations we set the Fermi level to zero.

where  $V$  is the volume of the unit cell and  $P$  is the hydrostatic pressure at that volume. Note that the energy  $E(\{e_i\})$  is the energy of the unit cell with the primitive vectors fixed, but any free atomic (internal) coordinates must be adjusted to minimize the total energy.

Since the  $\alpha$ -Sn (diamond) structure has a cubic lattice, there are only three independent elastic constants  $C_{11}$ ,  $C_{12}$  and  $C_{44}$ , with the bulk modulus (10) related to the elastic constants by

$$B = \frac{1}{3}(C_{11} + 2C_{12}). \quad (12)$$

The strain parameters needed to calculate these elastic constants are shown in table 3. Note that in the diamond structure the calculation of the bulk modulus and  $C_{11} - C_{12}$  requires no relaxation of the atomic positions, but the calculation of  $C_{44}$  requires the relaxation of one internal coordinate.

The  $\beta$ -Sn structure is tetragonal; so there are six independent elastic constants:  $C_{11}$ ,  $C_{12}$ ,  $C_{13}$ ,  $C_{33}$ ,  $C_{44}$  and  $C_{66}$ . The bulk modulus can be found by the relationship

$$B = \frac{(C_{11} + C_{12})C_{33} - 2C_{13}^2}{C_{11} + C_{12} - 4C_{13} + 2C_{33}}. \quad (13)$$

The strains needed to calculate these elastic constants are described in table 4. Several of these strains also require internal relaxations.

Introduction of the elastic strains  $\{e_i\}$  may reduce the symmetry of the crystal. For each strain, tables 3 and 4 show the space group of the resulting crystal, and the Wyckoff notation of the atomic positions (Hahn 1983)†.

We evaluated the elastic constants of  $\alpha$ -Sn at the experimental lattice constant, 12.26 Bohr. Our results are compared with experiment (Slutsky and Garland 1959) in table 5. The agreement with experiment is excellent.

The elastic constants of  $\beta$ -Sn are also computed at the experimental volume. Table 6 compares our results to an average of experimental room-temperature values (Simmons and Wang 1971). The agreement here is not as good as in table 5 largely

Table 3. The strain parameters needed to generate the elastic constants of tin in the diamond structure. For each strain we also list the space group of the strained lattice (Hahn 1983), the Wyckoff notation for the atomic positions, and the number of internal parameters which must be varied to obtain the relaxed structural energy.

Elastic constant	Strain parameters	Space group	Wyckoff notation	Number of internal parameters
$B$ (equation (12))	See text	$Fd\bar{3}m(O_h^7)$	8a	0
$C_{11} - C_{12}$	$e_1 = x$ $e_2 = -x$ $e_3 = x^2(1 - x^2)^{-1}$	$Fddd(D_{2h}^{24})$	8a	0
$C_{44}$	$e_6 = x$ $e_3 = x^2(4 - x^2)^{-1}$	$Imma(D_{2h}^{28})$	4e	1

† Space group operations and Wyckoff positions may also be obtained from the Bilbao Crystallographic Server at <http://www.cryst.ehu.es/>.

Table 4. The strain parameters needed to generate the elastic constants of tin in the  $\beta$ -Sn structure. For each strain we also list the space group of the strained lattice (Hahn 1983), the Wyckoff notation for the atomic positions, and the number of internal parameters which must be varied to obtain the relaxed structural energy.

Elastic constant	Strain parameters	Space group	Wyckoff notation	Number of internal parameters
$B$ (equation (13))	See text	$I4_1/amd(D_{4h}^{19})$	0	
$C_{11} + C_{12}$ $-4C_{13} + 2C_{33}$	$e_{1,2} = (1+x)^{-1/3} - 1$ $e_3 = (1+x)^{2/3} - 1$	$I4_1/amd(D_{4h}^{19})$	4a	0
$C_{33}$	$e_3 = x$	$I4_1/amd(D_{4h}^{19})$	4a	0
$C_{11}$	$e_1 = x$	$Imma(D_{2h}^{28})$	4e	1
$C_{11} - C_{12}$	$e_1 = -e_2 = x$ $e_3 = x^2(1-x^2)^{-1}$	$Imma(D_{2h}^{28})$	4e	1
$C_{44}$	$e_4 = x$ $e_3 = \frac{1}{4}x^2$	$C2/m(C_{2h}^3)$	4i	2
$C_{66}$	$e_6 = x$ $e_3 = x^2(4-x^2)^{-1}$	$Fddd(D_{2h}^{24})$	8a	0

Table 5. The elastic constants of  $\alpha$ -Sn calculated using the methods of Mehl (1993) modified for the diamond structure, as outlined in §4.1. Elastic constants were determined at the experimental room-temperature lattice constant, 12.26 Bohr, using the case-2 TB parameters. The experimental results are from Slutsky and Garland (1959).

	TB	Experiment
$B$ (GPa)	$42.6 \pm 1.0$	$46.53 \pm 0.5$
$C_{11} - C_{12}$ (GPa)	$37.6 \pm 0.7$	$30.24 \pm 1.1$
$C_{11}$ (GPa)	$67.7 \pm 1.5$	$66.67 \pm 0.7$
$C_{12}$ (GPa)	$30.1 \pm 1.2$	$36.45 \pm 0.4$
$C_{44}$ (GPa)	$38.0 \pm 1.0$	$30.20 \pm 0.2$

because we have not included a large amount of information about the LAPW  $\beta$ -Sn results in the fit. We note that, in spite of the fact that  $C_{13}$  may be negative, our TB elastic constants are consistent with the fact that the  $\beta$ -Sn structure is a metastable state.

We calculated phonon frequencies for  $\alpha$ -Sn by the frozen-phonon method (Klein and Cohen 1992), using supercells and displacements generated by the FROZSL package†. The results are compiled in table 7, where they are also compared with experiment (Price *et al.* 1971). Our TB Hamiltonian consistently overestimates the phonon frequencies of  $\alpha$ -Sn. These results could be substantially improved by performing some first-principles calculations, for example of the Raman frequency at  $\Gamma$ , and including the results in the fitting database.

† L. L. Boyer and H. T. Stokes provided the FROZSL code.

Table 6. Elastic constants of  $\beta$ -Sn, using the case-2 TB parameters and computed at the TB equilibrium volume, compared with an average of room-temperature experimental values (Simmons and Wang 1971).

	TB	Experiment
B (GPa)	98	53
$C_{11}$ (GPa)	$122 \pm 32$	$78 \pm 6$
$C_{12}$ (GPa)	$67 \pm 71$	$45 \pm 16$
$C_{13}$ (GPa)	$-24 \pm 35$	$33 \pm 7$
$C_{33}$ (GPa)	$210 \pm 12$	$100 \pm 19$
$C_{44}$ (GPa)	$22 \pm 4$	$27 \pm 13$
$C_{66}$ (GPa)	$38 \pm 1$	$26 \pm 17$

Table 7. Phonon frequencies of  $\alpha$ -Sn at the experimental lattice constant, calculated using the case-2 TB parameters and compared with experiment (Price *et al.* 1971). Frequencies are computed within the frozen-phonon approximation (Klein and Cohen 1992) using supercells and displacements generated by the FROZSL code.

	Frequency (THz)	
	TB	Experiment
$\Gamma$ (0, 0, 0)	7.29	6.00
$X_1$	5.42	4.67
$X_3$ ( $2\pi/a$ , 0, 0)	1.51	1.25
$X_4$	7.35	5.51
$L_1$	7.29	4.89
$L'_2$ ( $\pi/a, \pi/a, \pi/a$ )	3.27	4.15
$L_3$	1.33	1.00
$L'_3$	7.37	5.74

#### 4.4. Molecular dynamics

The NRL-TB method is sufficiently compact to make molecular dynamics calculations feasible on a high-performance multiprocessing supercomputer. Using the tight-binding molecular dynamics code (TBMD) (Kirchhoff *et al.* 2001) we performed calculations on supercells containing 686 atoms of tin in the diamond structure, using the case-2 parameters. The unit cell was fixed, with the atoms allowed to move freely in the unit cell subject to periodic boundary conditions. Typical calculations ran for 2000 time steps, at 2 fs per time step. The first 1000 time steps were used to equilibrate the system, and the remaining time steps were used in computing thermal averages. Given the finite system size, this method results in temperature fluctuations around the target temperature. Thus a typical 150 K simulation had an average temperature of 149 K, with a standard deviation of 12 K, and a 500 K simulation had an average temperature of 494 K and a standard deviation of 24 K.

Figure 6 shows the averaged electronic DOS of  $\alpha$ -Sn at a density corresponding to the fcc lattice constant of 12.261 Bohr, and at several temperatures between 150

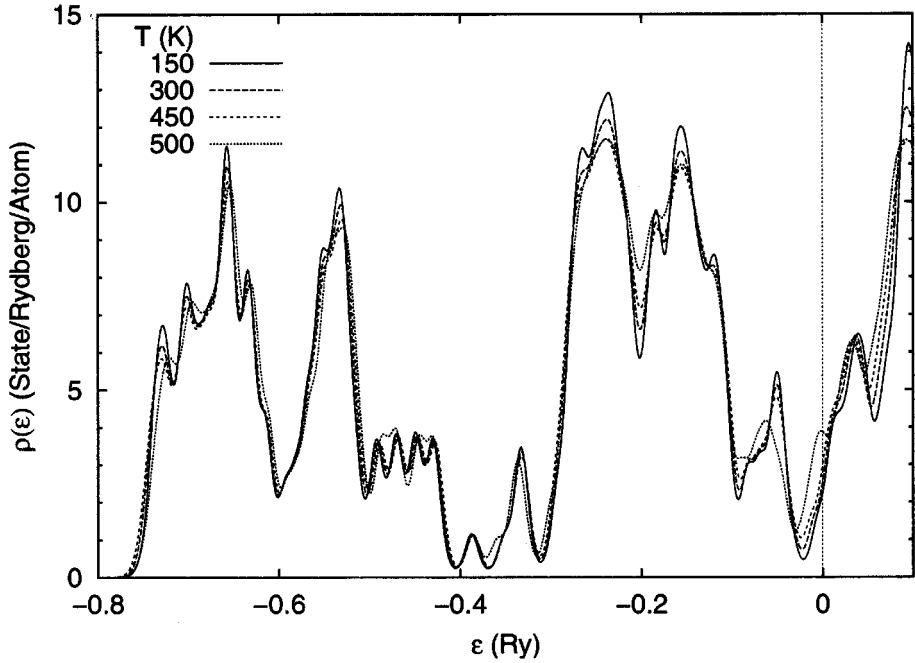


Figure 6. The thermally averaged electronic DOSs of  $\alpha$ -Sn, using the case-2 TB parameters, calculated using a 686-atom supercell at a density corresponding to an fcc lattice constant of 12.26 Bohr. The energies have been shifted so that  $\epsilon = 0$  corresponds to the static lattice Fermi level.

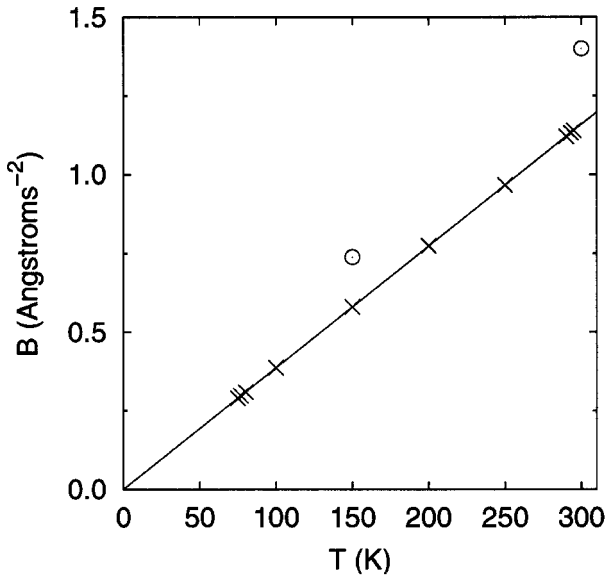


Figure 7. The Debye-Waller factor  $B$ , computed from our TBMD simulations ( $\circ$ ) via equation (14) and compared with experiment ( $\times$ ) (Peng *et al.* 1996): (—), linear fit to the experimental data.

and 500 K. We see a smearing of the DOSs in the pseudogap near the Fermi level, and a shift of the minimum of the DOS away from the Fermi level.

Finally, we have used the TBMD to compute the mean square deviation of the atoms. This is connected to the Debye–Waller factor  $B$  by the relation (Peng *et al.* 1996)

$$B = 8\pi^2 \langle u_x^2 \rangle = \frac{8}{3}\pi^2 \langle |\mathbf{r}|^2 \rangle, \quad (14)$$

where  $\langle u_x^2 \rangle$  is the thermal average of the mean square displacement in the  $x$  direction. By symmetry, this is just one third of the total mean square displacement of the atoms,  $\langle |\mathbf{r}|^2 \rangle$ . We compare our results with experiment (Peng *et al.* 1996) in figure 7. Up to room temperature, our results are consistent with the experimental data.

### § 5. SUMMARY

The NRL-TB method has been successful in describing the two known low-pressure stable structures of tin, the  $\alpha$ -Sn (grey) phase below 13°C and zero pressure and the  $\beta$ -Sn (white) phase at atmospheric pressure above 13°C. The bulk TB properties were found to be in excellent agreement with experiment and first-principles calculations for all the phases. The calculated band structures correctly predict a semiconductor with zero gap in the  $\alpha$ -Sn crystal structure, and a metal in the bcc structure. We correctly predict the phase transition sequence  $\alpha$ -Sn  $\rightarrow$   $\beta$ -Sn  $\rightarrow$  bct, but we cannot distinguish the bct  $\rightarrow$  bcc transition. The calculated TB Raman and zone-boundary phonon frequencies are consistently higher than experiment. Our molecular dynamics simulations are consistent with experiment, as evidenced by the behaviour of the Debye–Waller  $B$  factor as a function of temperature.

In conclusion, the present work has expanded the range of materials to which the NRL-TB method has been applied successfully, suggesting that its extension to more complicated structures and to binary compounds will produce satisfactory results as well.

### ACKNOWLEDGEMENTS

D.A.P. and M.J.M. were supported by the US Office of Naval Research. Development of the NRL-TB codes (Kirchhoff *et al.* 2001) was partially supported by the US Department of Defense Common High Performance Computing (HPC) Software Support Initiative. This work was supported in part by a grant of HPC time from the US Department of Defense Aeronautical Systems Center, Wright–Patterson Air Force Base, Dayton, Ohio, for computations on the IBM SP2 and SGI Origin. We wish to thank L. L. Boyer and H. T. Stokes for the use of their FROZSL package. We also wish to thank N. Bernstein for help in interpreting the results of the molecular dynamics simulations, and J. Feldman for providing us with a copy of the paper by Peng *et al.* (1996).

### REFERENCES

- ANDERSEN, O. K., 1975, *Phys. Rev. B*, **12**, 3060.  
 BERNSTEIN, N., MEHL, M. J., PAPACONSTANTOPOULOS, D. A., PAPANICOLAOU, N. I., BAZANT, M. Z., and KAXIRAS, E., 2000, *Phys. Rev. B*, **62**, 4477.  
 BIRCH, F., 1978, *J. Geophys. Res.*, **83**, 1257.  
 CHRISTENSEN, N. E., and METHFESSEL, M., 1993, *Phys. Rev. B*, **48**, 5797.  
 COHEN, R. E., MEHL, M. J., and PAPACONSTANTOPOULOS, D. A., 1994, *Phys. Rev. B*, **50**, 14 694.  
 DESGRENIERS, S., VOHRA, Y. K., and RUOFF, A. L., 1989, *Phys. Rev. B*, **39**, 10 359.

- DONOHUE, J., 1974, *The Structures of the Elements* (New York: Wiley), pp. 272–278.
- HAHN, T. (editor) 1983, *International Tables for Crystallography*, Vol. A (Dordrecht: Reidel).
- HEDIN, L., and LUNDQVIST, B. L., 1971, *J. Phys. C*, **4**, 2064.
- HOHENBERG, P., and KOHN, W., 1964, *Phys. Rev. B*, **136**, B864.
- KIRCHHOFF, F., MEHL, M. J., PAPANICOLAOU, N. I., PAPACONSTANTOPOULOS, D. A., and KHAN, F. S., 2001, *Phys. Rev. B*, **63**, 195 101.
- KLEIN, B. M., and COHEN, R. E., 1992, *Phys. Rev. B*, **45**, 12 405.
- KOELLING, D. D., and ARBMAN, G. O., 1975, *J. Phys. F*, **5**, 2041.
- KOELLING, D. D., and HARMON, B. N., 1977, *J. Phys. C*, **10**, 3107.
- KOHN, W., and SHAM, L. J., 1965, *Phys. Rev. B*, **140**, A1133.
- MEHL, M. J., 1993, *Phys. Rev. B*, **47**, 2493.
- MEHL, M. J., KLEIN, B. M., and PAPACONSTANTOPOULOS, D. A., 1994, *Intermetallic Compounds—Principles and Practice*, Vol. 1, edited by J. H. Westbrook and R. L. Fleischer (London: Wiley), chapter 9, pp. 195–210.
- MEHL, M. J., and PAPACONSTANTOPOULOS, D. A., 1995, *Europhys. Lett.*, **31**, 537; 1996, *Phys. Rev. B*, **54**, 4519.
- OLIJNYK, H., and HOLZAPFEL, W. B., 1984, *J. Phys. Paris*, **45**, Suppl. 11, C8–153.
- PAPACONSTANTOPOULOS, D. A., 1986, *Handbook of Electronic Structure of Elemental Solids* (New York: Plenum).
- PAPACONSTANTOPOULOS, D. A., MEHL, M. J., ERWIN, S. C., and PEDERSON, M. R., 1998, *Tight-Binding Approach to Computational Materials Science*, Materials Research Society Symposium Proceedings, Vol. 491, edited by P. Turchi, A. Gonis and L. Colombo (Pittsburgh, Pennsylvania: Materials Research Society), p. 221.
- PENG, L.-M., REN, G., DUDAREV, S. L., and WHELAN, M. J., 1996, *Acta crystallogr. A*, **52**, 456.
- PERDEW, J. P., 1991, *Electronic Structure of Solids '91*, edited by P. Ziesche and H. Eschrig (Berlin: Akademie), p. 11.
- PRICE, D. L., ROWE, J. M., and NICKLOW, R. N., 1971, *Phys. Rev. B*, **3**, 1268.
- SIGALAS, M. M., and PAPACONSTANTOPOULOS, D. A., 1994, *Phys. Rev. B*, **49**, 1574.
- SIMMONS, G., and WANG, H., 1971, *Single Crystal Elastic Constants and Calculated Aggregate Properties: A Handbook*, second edition (Cambridge, Massachusetts: MIT Press).
- SINGH, D., 1991, *Phys. Rev. B*, **43**, 6388.
- SLATER, J. C., and KOSTER, G. F., 1954, *Phys. Rev.*, **94**, 1498.
- SLUTSKY, L. J., and GARLAND, C. W., 1959, *Phys. Rev.*, **113**, 167, and references therein.
- VILLARS, P., and CALVERT, L. D. (editors), 1991, *Pearson's Handbook of Crystallographic Data for Intermetallic Phases*, second edition (Materials Park, Ohio: American Society for Metals).
- WEI, S. H., and KRAKAUER, H., 1985, *Phys. Rev. Lett.*, **55**, 1200.
- YANG, S. H., MEHL, M. J., and PAPACONSTANTOPOULOS, D. A., 1994, *Phys. Rev. B*, **57**, R2013.